Received: 6 May 2019 | Revised: 15 October 2019 | Accepted: 22 October 2019

DOI: 10.1002/pc.25425

Check for updates

RESEARCH ARTICLE

spe INSPIRING PLASTICS PROFESSIONALS Polymer COMPOSITES WILEY

Film formation and mechanical properties of an opaque titanium dioxide and transparent polyvinyl alcohol composite films

Altan Bozdoğan | **Baki Aksakal** | **Onder Yargi**

Department of Physics, Yıldız Technical University, Esenler, İstanbul, Turkey

Correspondence
Altan Bozdoğan, Department of Physics, Yıldız Technical University, Esenler 34210, İstanbul, Turkey.
Email: abozdog@yildiz.edu.tr

Funding information
Scientific Research Projects Coordinatorship, Grant/Award Number: 2016-01-01-GEP02

Abstract

Mechanical, optical, and film formation properties of titanium dioxide/polyvinyl alcohol (TiO_2/PVA) composites were studied. Two identical experimental sets of % TiO_2 content were prepared that one set is in the range of 1, 3, 5, 7, 10, 13, and 20 wt% for the film formation and the second set is 5 and 50 wt% for the mechanical measurements. Photon transmission technique (PT) at room temperature was used for the film formation process after annealing for 10 min at the temperatures changing from 100 to 270°C. The increase and decrease in the transmission light intensity (I_{tr}) from the composite films were attributed to void closure and interdiffusion models, respectively. The results were consistent with the data obtained from the film formation processes and mechanical measurements that the addition of TiO_2 in PVA had remarkable improvement on mechanical properties, for example, increment in the Young's modulus and the rigidity as TiO_2 content increased from 5 to 50 wt%, and it had also good film forming especially above 10 wt% TiO_2 for the void closure processes leading to lower the activation energy. It was observed that for the lower content of TiO_2 such as 5 wt%, the tensile strength and Young's modulus increased remarkably for heating temperature increased up to 150°C. However, with the increase of TiO_2 content, the maximum values of the mechanical strength and modulus were shifted to 180°C for 50 wt% TiO_2 from 150°C for 5 wt% TiO_2 because of the thermal stability of TiO_2.

KEYWORDS

films, FT-IR, mechanical properties, thermal properties, UV-visible spectroscopy

1 | INTRODUCTION

As a result of worldwide theoretical and experimental efforts, a very good understanding of the mechanisms of latex film formation has been achieved.[1–4] The film formation from soft (low-T_g) and hard (high-T_g) latex dispersions can occur in several stages. In both cases, the first stage corresponds to the wet initial stage. Evaporation of solvent leads to second stage in which the particles form a close packed array. Here, if the particles are soft, they are deformed to polyhedrons. However, hard latex stays undeformed at this stage. Annealing of soft particles causes diffusion across particle-particle boundaries, which lead to a homogeneous continuous material. In the annealing of hard latex system, however, the deformation of particles first leads to void closure[1–4] and then, after the voids disappear, diffusion across particle-particle boundaries starts, that is, the mechanical properties of hard latex films evolve during annealing; after all solvent is evaporated and all voids are disappeared.

 © 2019 Society of Plastics Engineers

Transmission electron microscopy (TEM) has been the most common technique used to investigate the structure of the dried films.[5,6] The pattern of hexagons, consistent with face-centered cubic packing, is usually observed in highly ordered films. When these films are annealed, complete disappearance of structure is sometimes observed, which is consistent with extensive polymer interdiffusion. Freeze fracture TEM (FFTEM) has been used to study the structure of dried latex films.[7] Small angle neutron scattering (SANS) has been used to study latex film formation at molecular level. Extensive studies using SANS have been performed by Sperling and coworkers[8] on compression-molded polystyrene film. Direct-nonradiative energy transfer (DET) method has been employed to investigate the film formation process from dye-labeled hard[9] and soft[10,11] polymeric particles. The steady state fluorescence technique combined with DET has been used to examine healing and interdiffusion processes in the dye-labeled poly(methyl methacrylate) (PMMA) latex systems.[12–14] Recently, UV-Visible (UVV) technique has been used to study film formation from reduced graphene oxide (rGO) and PVA[3] where the transmitted light intensity was monitored during film formation process. This latex film formation[15,16] can now be exploited to underpin the processing of new types of coatings and development of new materials. The blending of latex particles and inorganic nanoparticles provides a facile means of ensuring dispersion at the nanometer scale in composite coatings. In last decade, there has been growing interest on producing new materials by filling polymers with inorganic natural and/or synthetic compounds. These composite materials possess high heat resistance, mechanical strength, and impact resistance or present weak electrical conductivity and low permeability for gases like oxygen or water vapor.

TiO_2 has an extraordinary stability, hydrophobicity, UV absorbance, high refractive index, nontoxicity, and excellent transparency for the visible light. Also, TiO_2 has a strong redox ability, thus, it is used for photo electrochemical cell.[17] The immobilization of TiO_2 nanoparticles on transparent substrates such as PVA will be an efficient approach to improve the photocatalytic activity. PVA is a water-soluble polymer, which is widely used as functional membranes with high transparency.[18] Beside the transparency, it has also a good film forming, physical properties, a good process ability, biocompatibility, and a good chemical resistance. To further enhance the properties of this polymer, the addition of an inorganic material is advantageous for forming a composite, which could be lightweight, flexible, and exhibit a good moldability.[19]

In this work, film formation, optical, and mechanical properties of high-T_g of TiO_2 and low-T_g of PVA composites were studied. The film formation process of the films was carried out by UVV technique. In addition to the differences between glass transition of TiO_2 and PVA, the opacity effect of TiO_2 on the transparent PVA substrate was also studied in terms of optical properties. Beside the help of spectral analysis, the results of film formation process of TiO_2/PVA composite films were used to understand the changes in mechanical properties of composite films heated at various temperatures.

2 | EXPERIMENTAL

2.1 | Materials

2.1.1 | Preparation of TiO_2/PVA solution

The PVA used in the production of pure PVA and TiO_2/PVA composite films was obtained from Boysan Co., Turkey. It has powder form and white color, water soluble and its pH value is at around 4.5 to 6.5 and it includes acetic acid ethenyl ester, polymer with ethanol, 92% to 100%. TiO_2 particles were obtained from Nanografi Co., Turkey. It has also powder form, white color, water soluble and pH value at around 5.5 to 6.5, true density 4.1 g/cm^3 and the average particle size of 28 nm. TiO_2 solution was prepared at room temperature in the following way: 0.0028 g/ml titanium (Rutile) dioxide was injected slowly in 15 ml ethanol. A few drops of acetic acid was added and stirred for half an hour. Later, 10 ml ethanol was added to this mixture and stirred for 1 h. PVA distribution was prepared by mixing at 60°C temperature in distilled water for 1 h.

2.1.2 | Preparation of TiO_2/PVA composite films

Two sets were prepared from the dispersion of TiO_2/PVA composites by placing the same number of drops on a glass plates with the size of 0.8×2.5 cm^2 and allowing the water to evaporate. One set was prepared for the film formation process and the other set was prepared for the mechanical measurements. Then, the samples were separately annealed starting from 90°C below T_g of PVA to 270°C for 10 min in an oven. The temperature was maintained with ±2°C during annealing inside the oven.

2.2 | Methods

2.2.1 | Photon transmission measurements

Photon transmission experiments were performed using B&W Tek spectrometer. The transmittances of the films were detected at 800 nm. A glass plate was used as a standard

for all UVV experiments, and the measurements were performed at room temperature after each annealing processes.

2.2.2 | Tensile testing method

Uniaxial tensile tests of PVA and the prepared composite films were carried out by using a Llyod tensile testing machine LF plus (AMETEK Lloyd, UK) with a crosshead speed of 20 mm min^{-1} at room conditions (T = 25°C; RH = 60%). The initial gauge length of the samples was chosen as 20 mm and the test specimens had the same width of 4 mm, and varying film thicknesses from 35 ± 5 to 100 ± 5 μm measured by using a digital micrometer (Mitutoyo, No. 293-821-30, Japan). The data reported here were averaged over at least 6 to 8 specimens. In order to investigate the influence of heating on the stress-strain behavior of pure PVA, 5 and 50 wt% TiO_2 doped PVA composites, the films were annealed at 150, 180, and 210°C for 10 min in the temperature chamber. Then, unheated and heated films were tested by using the tensile tester at ambient temperature.

2.2.3 | FT-IR/ATR spectroscopic method

The FT-IR/ATR spectroscopic measurements were obtained on a Thermo Scientific Nicolet iS5 FT-IR Spectrometer equipped with a iD7 ATR sampling accessory. The spectra of the unheated and heated samples were recorded in the wavenumbers ranging from 4000 to 400 cm^{-1} at a resolution of 4 cm^{-1} with 32 scans for each measurement at room conditions.

2.2.4 | Energy dispersive spectroscopy

The energy dispersive spectroscopy (EDS) measurements were performed by Quanta Scanning Electron Microscope (model FEG 450) equipped with energy dispersive spectrometer. The element analysis of the untreated TiO_2/PVA composite films with TiO_2 (wt%) at 3 and 20 were performed between applied voltage of 0 to 16 keV.

3 | RESULTS AND DISCUSSION

3.1 | Mechanical properties of TiO_2/PVA composite films

By using the results of the mechanical measurements, the influence of heating on the stress-strain behavior and corresponding tensile characteristics of pure PVA, 5, and 50 wt% TiO_2 doped PVA composite films were given in Table 1 and Figure 1.

It is clear that with the addition of TiO_2 nanoparticles with ratio of 5 wt%, prominent changes were seen on the strain at break value as well as a small decrease in the Young's modulus and the tensile strength of pure PVA films. Because low amount of TiO_2 nanoparticles have weak intermolecular interaction with PVA molecules, as the TiO_2 content increased up to 50 wt%, the important reinforcement effect on the Young's modulus and rigidity were seen. It is thought that the increase in the Young's modulus and the rigidity are due to the strong adhesion and interactions between some of the added TiO_2 nanoparticles and the PVA matrix via the formation of Ti—O—C covalent bonds between TiO_2 and PVA cites. Although TiO_2 nanoparticles break the intermolecular hydrogen bonding between the PVA polymer chains as illustrated in Figure 2, because TiO_2 molecules form Ti—O—C bond, they lead to an increase in the rigidity of the PVA polymer chains. Besides, due to excessive amount of TiO_2 nanoparticles, it may be concluded that noninteracting TiO_2 particles with PVA molecules can form TiO_2 clusters themselves, which lead to a contribution to rigidity because of their high rigidity and Young's

TABLE 1 Influence of heating on uniaxial tensile properties of pure PVA, 5, and 50 wt% TiO_2 doped PVA composite films

	Temperature (°C)	E_Y (MPa)	σ_T (MPa)	ε_b (%)	W_b (J)
Pure PVA	20	55.09	19.29	350.43	0.19635
5 wt% TiO_2/PVA	20	16.28	17.94	470.59	0.30146
	150	651.72	33.53	200.72	0.42365
	180	463.08	30.80	197.58	0.27268
	210	416.92	16.26	183.39	0.22479
50 wt% TiO_2/PVA	20	261.78	8.03	27.94	0.01216
	150	548.34	10.55	11.27	0.00456
	180	1226.94	14.72	13.81	0.00605
	210	984.04	8.49	6.65	0.00225

Abbreviations: E_Y, Young's modulus; PVA, polyvinyl alcohol; W_b, work to break; ε_b, strain at break; σ_T, tensile strength.

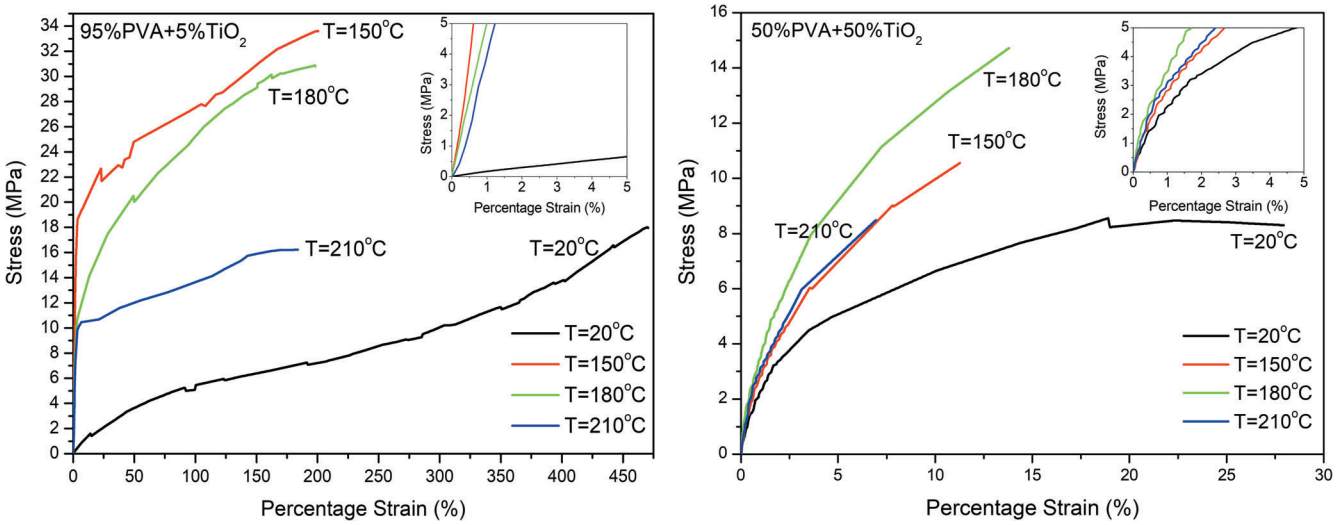


FIGURE 1 The influence of heating on stress-strain curves of 5 and 50 wt% TiO_2/PVA composite films [Color figure can be viewed at wileyonlinelibrary.com]

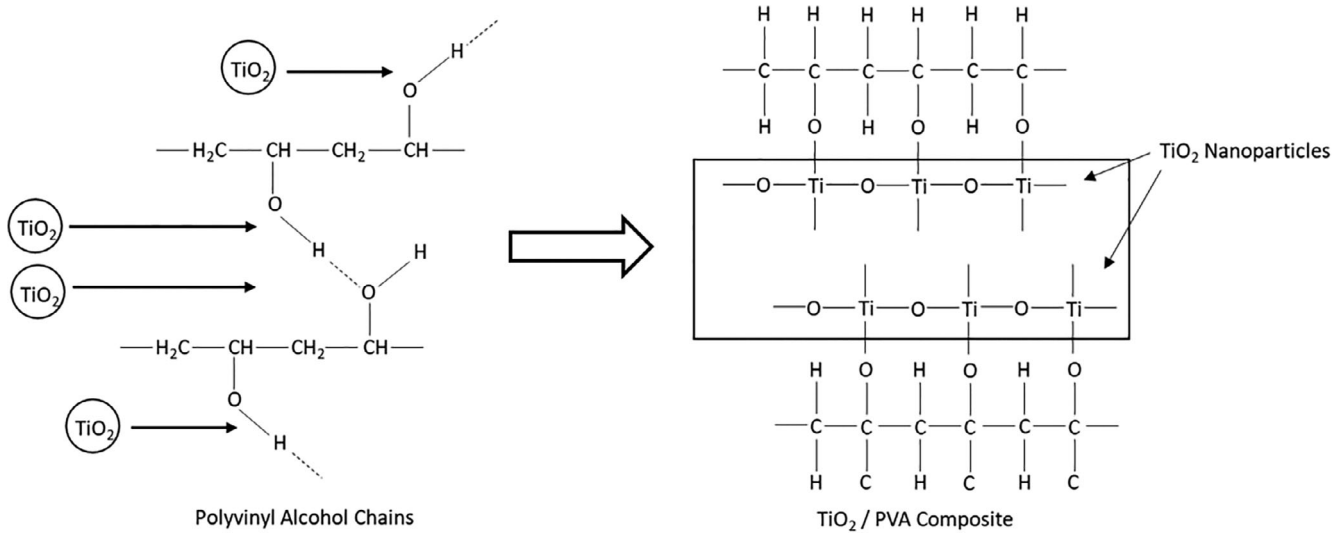


FIGURE 2 Schematic representation of possible interaction between TiO_2 nanoparticles and PVA chains

modulus at around 250 GPa. It should be emphasized that due to high content and high mechanical characteristics of TiO_2, the dominant effect of TiO_2 was seen on the mechanical properties of TiO_2/PVA composite films.

When we compared the influence of heating on the mechanical characteristic of TiO_2/PVA composites, it was seen in Figure 3 that the tensile strength increased significantly as the anneal temperature increased up to around 180°C for both 5 and 50 wt% TiO_2-PVA composite films.

It is also seen in Figure 4 that Young's modulus of 5 wt% TiO_2/PVA composite films increased around 40 times at 150°C compared with that of unheated sample. However, it should be noticed that the anneal temperature for which the Young's modulus obtained maximum value shifted to 180°C from 150°C as TiO_2 content increased from 5 to 50 wt% in the composite film. Because the thermal stability of TiO_2 is higher than PVA, although thermal degradation starts at around 180°C for the 5 wt% TiO_2/PVA composite, the composite film with 50 wt% TiO_2 content started to degrade for the anneal temperature higher than around 180°C. As the annealing temperature increased, intermolecular interactions and the formation of Ti—O—C covalent bonds increased which leads to increase in the rigidity and decrease in the extensibility of the composite films, because the present water molecules adsorbed on the surfaces of TiO_2 nanoparticles and also free water molecules in the structure of PVA can evaporate. As the annealing temperature increased, the toughness and the energy required to break the sample in the tensile deformation decreased significantly. Severe thermal degradation generally started at the temperature above 200°C.

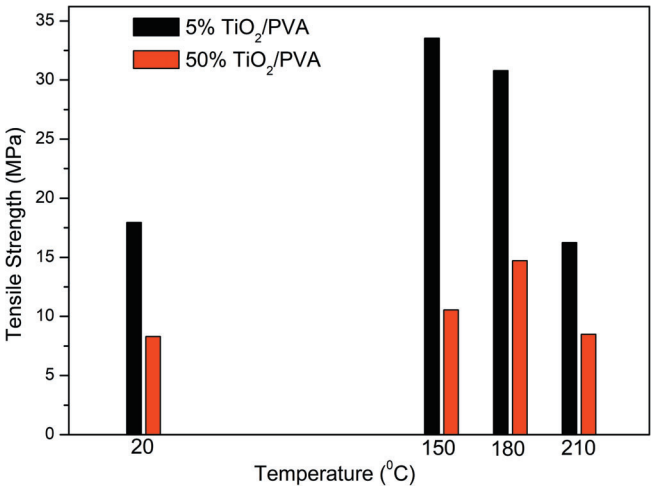


FIGURE 3 The influence of heating on tensile strength of 5 and 50 wt% TiO_2/PVA composite films [Color figure can be viewed at wileyonlinelibrary.com]

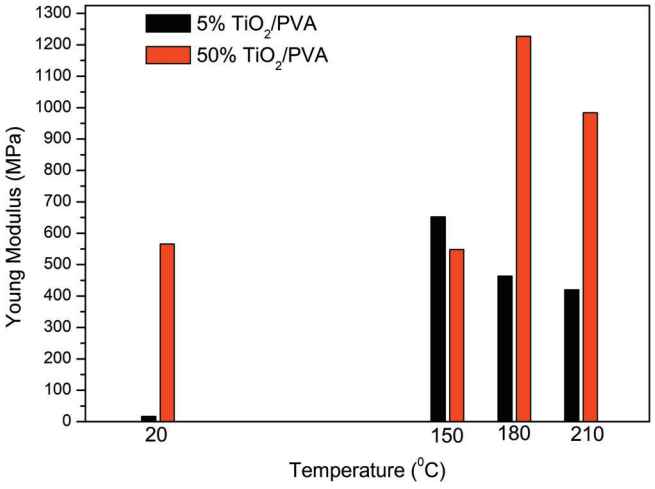


FIGURE 4 The influence of heating on the Young's modulus of 5 and 50 wt% TiO_2/PVA composite films [Color figure can be viewed at wileyonlinelibrary.com]

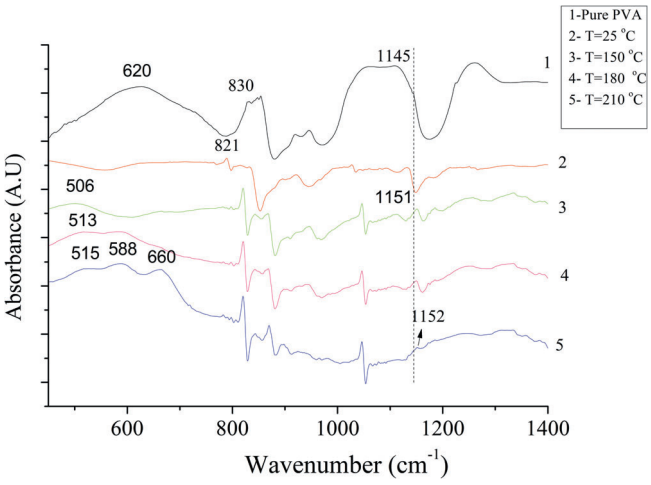


FIGURE 5 The influence of heating on the FT-IR spectra of 5 wt% TiO_2/PVA composite films in the wavenumber range of 450 to 1400 cm^{-1} [Color figure can be viewed at wileyonlinelibrary.com]

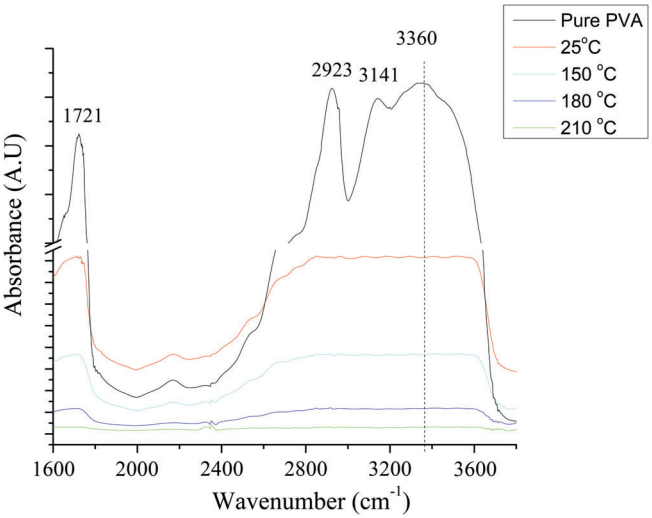


FIGURE 6 The influence of heating on the FT-IR spectra of 5 wt% TiO_2/PVA composite films in the wavenumber range of 1600 to 3800 cm^{-1} [Color figure can be viewed at wileyonlinelibrary.com]

3.2 | FT-IR/ATR spectral analysis

The FT-IR/ATR spectra of TiO_2/PVA composite films were recorded after the composite films were heated at different temperatures. Vertically translated spectra in the region of 450 to 1400 $cm^{-1}$of pure PVA and 5 wt% TiO_2/PVA films after heated at various temperatures were given in Figure 5. Similarly, Figure 6 shows the spectral region from 1600 to 3800 cm^{-1} of these samples.

Prominent band frequencies and their assignments in pure PVA films and TiO_2 were summarized in Table 2 by using the references in the literature.[20–55] Here, as it is seen in Figure 5, the spectral region where the band at around 620 cm^{-1} corresponding to out of plane OH bending[26] in pure PVA films was changed after the addition of TiO_2 nanoparticles into PVA films. Although they were not well marked for the unheated 5 wt% TiO_2/PVA films, some characteristic peaks of TiO_2, that is, the peaks at around 588 and 660 cm^{-1} assigned to the stretching mode of Ti—O—Ti bond[25] and a band at 506-515 cm^{-1}assigned to the vibration of Ti—O—O bond[20,21] or to Ti—O—Ti bond[22] were observed more clearly for heated samples at higher temperatures. Moreover, even though the symmetric (C—C) stretching mode in crystalline region of PVA which is considered as a crystallization sensitive band of PVA was observed at 1145 cm^{-1} for pure PVA films and it was shifted from

TABLE 2 The vibration frequencies and band assignments of the peaks observed in pure PVA films and TiO_2

Vibration frequency (cm^{-1})	Band assignment	References
515	Ti—O—O bond/Ti—O—Ti stretching	[20–22]
608	Out of plane (OH) bending	[23, 24]
685-800	Ti—O stretching	[20–22, 25]
580-660	Ti—O—Ti stretching	[22]
827, 849	C—C stretching	[23, 26]
916	Skeletal vibration of PVA	[27–29]
1089-1096	C—O stretching vibration	[27, 30–37]
1133, 1141	Crystallization sensitive band of PVA, symmetric C—C stretching	[20, 21, 26, 27, 31, 32, 38, 39]
1242, 1257	C—H Wagging	[23, 26, 27, 31, 40]
1329, 1340	CH + OH, the bending vibration of bond CO—H	[27, 30, 41, 42]
1374	Wagging of CH_2	[27, 43, 44]
1424	Symmetric bending mode of (CH_2)	[23, 26, 27, 30, 43, 44]
1712, 1740	C═O stretching vibration	[36, 37, 45–47]
2852	C—H stretching vibration	[23, 27]
2914	CH_2 symmetric vibration	[26, 27, 41, 48]
2939	CH_2 antisymmetric vibration	[26, 27, 41, 48]
3200-3570	Stretching vibration of H bonded hydroxyl group	[20, 26, 41, 48–50]
3450-3650	Nonbonded OH stretching	[50, 51]
3414-3490	OH stretching vibration of water molecules adsorbed on the surface of the nanoparticles (TiO_2)	[27, 52–55]

Abbreviation: PVA, polyvinyl alcohol.

1146 to 1152 $cm^{-1}$with reducing absorbance from 0.82 to 0.029 as heating temperature increased from 25 to 210°C for the 5 wt% TiO_2 composite films. Similarly, the band appeared at around 830 cm^{-1} corresponding to C—C stretching vibration was shifted to lower values like 821 cm^{-1} with the effect of TiO_2 addition. Here, the band position did not change considerably, but its absorbance value reduced as the heating temperature increased. Such great decrease in the absorbance of the C—C stretching vibrations can be due to the deformation of chemical bonds and of the motions of molecules and the thermal degradation with increasing heating temperature, because the thermal degradation can cause some bond breakages and increasing the thermal energy leads to the increase in the mobility of polymer chains in both crystalline and amorphous domains.

It is seen in Figure 6 that TiO_2 nanoparticles can affect the intermolecular interactions such as hydrogen bonding and form new bonds with OH groups of PVA molecules, thus, the spectral region of 3200 to 3650 cm^{-1}corresponding to OH stretching vibration was considerably affected. In pure PVA films, the broad peak from 3200 to 3570 cm^{-1} is assigned to the stretching vibration of H bonded hydroxyl group and the stretching vibration of nonbonded OH groups was observed at 3450 to 3650 cm^{-1}.[50,51] Therefore, as shown in Figure 6, the peak observed at around 3140 cm^{-1} may be assigned to the stretching vibration of H bonded OH groups in PVA, while another broad peak centered at around 3360 cm^{-1} can correspond to nonbonded OH stretching vibration. It was reported that in the spectrum of TiO_2, the peak at around 3414 to 3490 cm^{-1} was assigned to OH stretching vibration of water molecules adsorbed on the surface of the TiO_2 nanoparticles.[27,52–55] In the spectrum of 5 wt% TiO_2 films, because TiO_2 nanoparticles affect the OH spectral region significantly via intermolecular interactions of the OH groups of water molecules adsorbed on the surfaces of TiO_2 nanoparticles with PVA molecules, there appears a broad peak from around 2800 to 3600 cm^{-1} as seen in Figure 6.

After the samples were heated at various temperatures, the absorbance of stretching vibration of OH groups (A_{3360}) which do not form hydrogen bonding decreased significantly. In Figure 7, it is seen that with increasing anneal temperature, the absorbance (A_{3360}) decreased greatly. It is thought that after TiO_2 nanoparticles were added in to the PVA at room conditions, the significant decrease in the

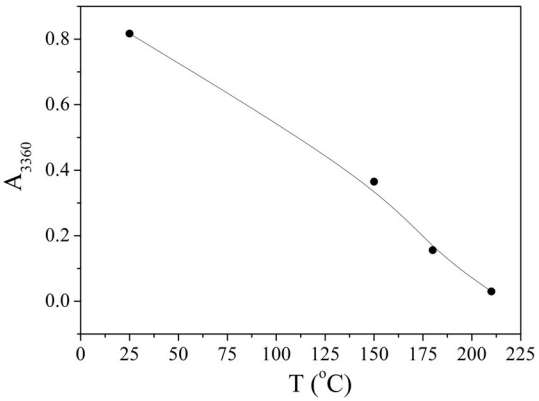


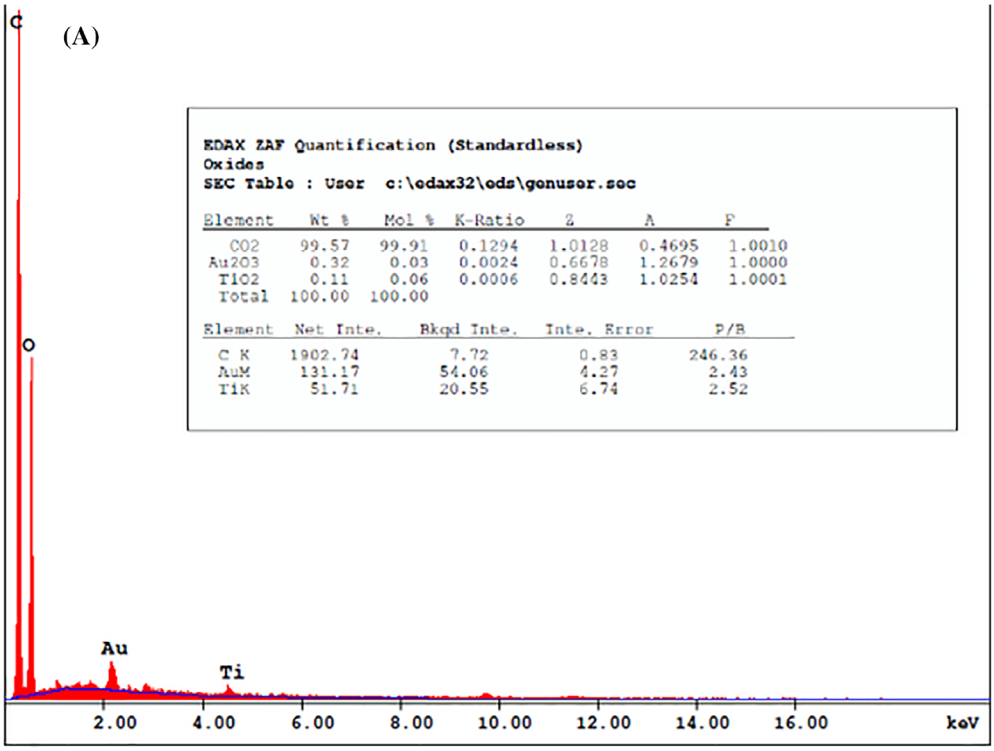
FIGURE 7 The effect of annealing temperature on the absorbance of the vibration of nonbonded OH groups of 5 wt% TiO_2/PVA composite films

absorbance of OH groups as seen in Figure 6 can be due to the formation of Ti—O—C covalent bonds with OH groups of PVA polymer chains in both crystalline and amorphous regions which increase the mechanical strength and the stiffness of the PVA structure. The further decrease in the absorbance of the stretching vibration of the OH groups with increasing anneal temperature and heating effect may be as a result of both the increase in the number of formations of Ti—O—C covalent bonds and the removal of the water molecules in the film structure.

3.3 | Film formation process of TiO_2/PVA composite films

The identification of Ti elements TiO_2/PVA composite films with TiO_2 content of 3 and 20 wt% in 3 and 20 wt% EDS technique was presented in Figure 8. It is clearly seen in Figure 8B that amount of Ti element is higher for the 20 wt% TiO_2 than that of Figure 8A (3 wt% TiO_2). Here, it should be noted that although the magnification was increased 600 000 times, SEM images of TiO_2 particles could not be clearly observed, because of very small particle size (28 nm). Thus, the unclear SEM images were not presented here.

From the results of phototransmission analysis, the transmitted light intensities, I_{tr} of 1, 3, 5, 7, 10, and 13 wt % TiO_2 content blend films annealed at various temperatures for 10 min are shown in Figure 9. All the curves in Figure 9 have the same characteristic behaviors that I_{tr} from all composites first increases by showing a maximum at a certain temperature called healing temperature, T_h. Then, because of further annealing, I_{tr} decreases again. The increase and decrease of I_{tr} upon annealing of these composite films can be explained with the void closure and interdiffusion processes, respectively.[1,2] Spherical particles that have increasing surface energy flow to voids (void closure) at the early stage of annealing, where the radius of interparticle voids becomes smaller and the film surface becomes more homogeneous; consequently, transparency of the film starts to increase. If the annealing process is carried on, chain segments (minor chains) move across the particle-particle interfaces, and therefore, the latex film becomes more transparent. This process is called *healing*. At high annealing temperatures, the chains gain sufficient kinetic energy to transform its center of mass across the junction surface (interdiffusion), and therefore, the latex film becomes fully transparent. The distribution of PVA having low-T_g moves toward the voids between TiO_2 particles with annealing of the composite films. Thus, the intensity of light passing through a film with less voids is higher since mean free path is rising between the films due to more homogenous structure. In other words, the films scattered less photons due to homogenization during the film formation. The decrease in the I_{tr} can be explained by the particles of TiO_2 among the homogeneously dispersed PVA distribution, that is, two medium with different refractive indices are randomly formed in the composite system. The scattering centers in the composite film are increased as TiO_2 amount is increased, thus, more light is scattered and, as a result, the optical transmission of the film is decreased. In other words, after T_h point, PVA starts to lose its effect and TiO_2 becomes dominant for the higher annealing temperatures for all composites. Having high-T_g of TiO_2 compared to the PVA starts to move which creates aggregation in the matrix and this leads more voids which scatter the light passing through the film resulting lower I_{tr}. Here, it should also be noted that the difference between the increasing and decreasing rates of I_{tr} can be seen clearly for 1 and 3 wt% TiO_2 where I_{tr} curves increase slowly at the beginning of annealing process. These findings are also consistent with the mechanical measurements that the tensile strength of TiO_2 particles are much higher than that of PVA distribution at 150 and 180°C and then decreasing again in Figure 9. These critical temperature values are the same behavior for the optical measurements that I_{tr} is increasing up to 150 to 180°C and starts to decrease above it for all composites in Figure 9. These indicate that the addition of TiO_2 into the PVA distribution plays an important role for determining of the film formation and the mechanical properties of composite films. Higher tensile properties of TiO_2 up to these temperatures show that it is more durable for the replacement of the particles in the matrix. Up to these temperature ranges, PVA is active and fills the voids both between the TiO_2 particles and clusters resulting high I_{tr}. Above that, TiO_2 starts to lose effect of the tensile strength and the particles start to move which act as scatter centers result lower I_{tr} in the matrix.



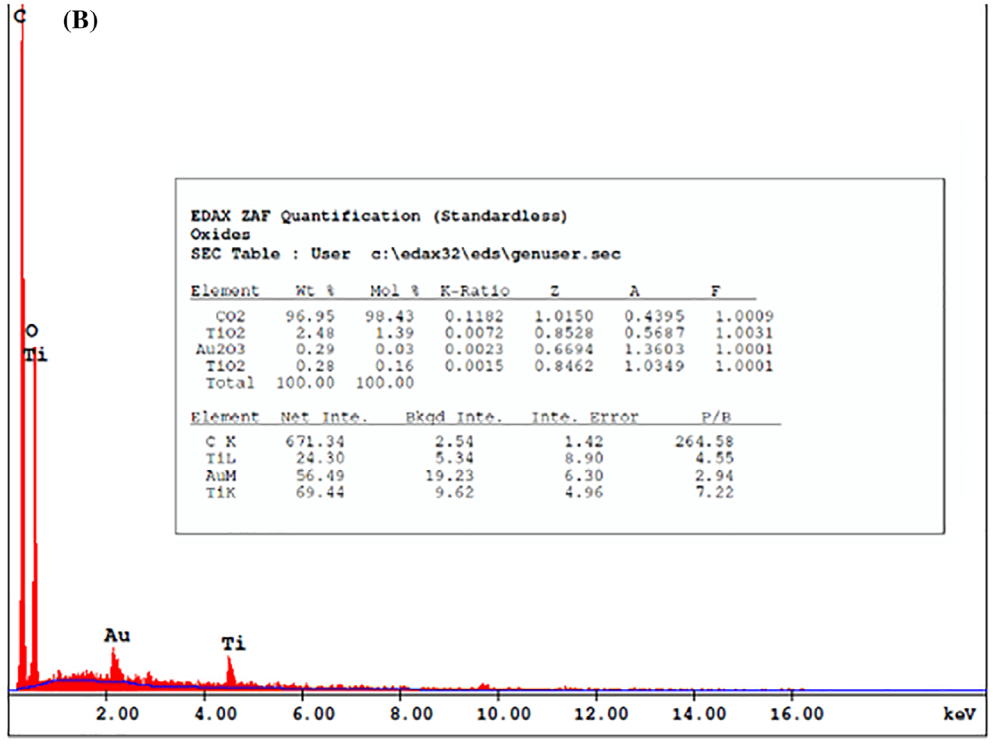


FIGURE 8 Identification of the Ti elements in (A) TiO_2/PVA composite films with TiO_2 content of 3 wt% and (B) TiO_2/PVA composite films with TiO_2 content of 20 wt% by EDS technique [Color figure can be viewed at wileyonlinelibrary.com]

3.4 | Calculation of the activation energies

The activation energies for the void closure and the interdiffusion processes are calculated by fitting the experimental data to the following equations[1]:

$$I_{tr}(T) = S(t)\exp\left(-\frac{3\Delta H}{kT}\right) \quad (1)$$

$$I_{tr}(T)/I_{tr}(\infty) = A\exp\left(-\frac{\Delta E}{2k_B T}\right), \quad (2)$$

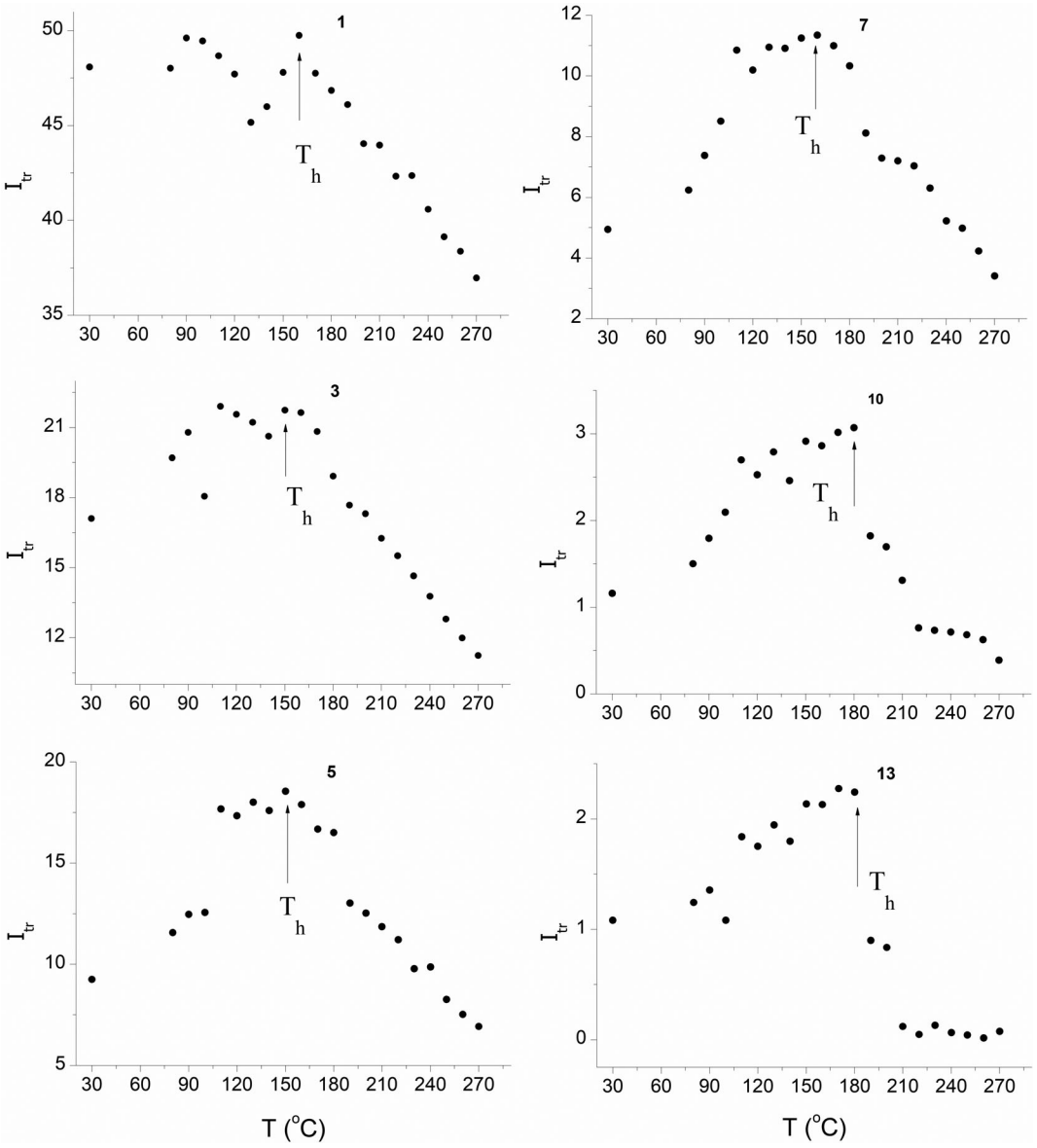


FIGURE 9 The change of the transmitted light intensities with temperature for different TiO_2 concentrations (1, 3, 5, 7, 10, and 13 wt%) in TiO_2/PVA composite films

where $S(t) = (yt/2\,AC)$,[3] k is the Boltzmann's constant, ΔH is the void closure energy, and I_{tr} is the transmittance at 800 nm.

As it was already argued earlier that the increase I_{tr} originates because of the void closure process, then Equation (1) was applied to I_{tr} below T_h for all film samples. The measured ΔH and ΔE activation energies are seen in Figure 10. Requiring force for the film formation depends on the inverse of the particle size, according to the descriptions of film formation driven by capillary forces.[2] The greater curvature and higher surface area of particles are expected to enhance the film formation. Activation energy of viscous flow is less with high PVA amount during void closure process where low temperatures are effective. Since PVA has lower T_g and higher surface area than TiO_2 sphericals, ΔH values are less than that of high TiO_2 amount in Figure 10A. The decrease in I_{tr} was already mentioned in above section, by the interdiffusion of polymer chains. As the annealing temperature is increased above maxima, some part of the polymer chains may cross the junction surface and particle boundaries disappear, as a result I_{tr} decreases because of transparency of the film.

It is seen that when TiO_2 content is added to the PVA, ΔE values are getting bigger up to a specific amount of PVA. It is attributed to the glass transition of the materials that PVA has lower T_g than that of TiO_2. Polymer chain transfer realizes at higher temperatures where TiO_2 is dominant. As it is seen from the Figure 10B that the replacement of TiO_2 particles

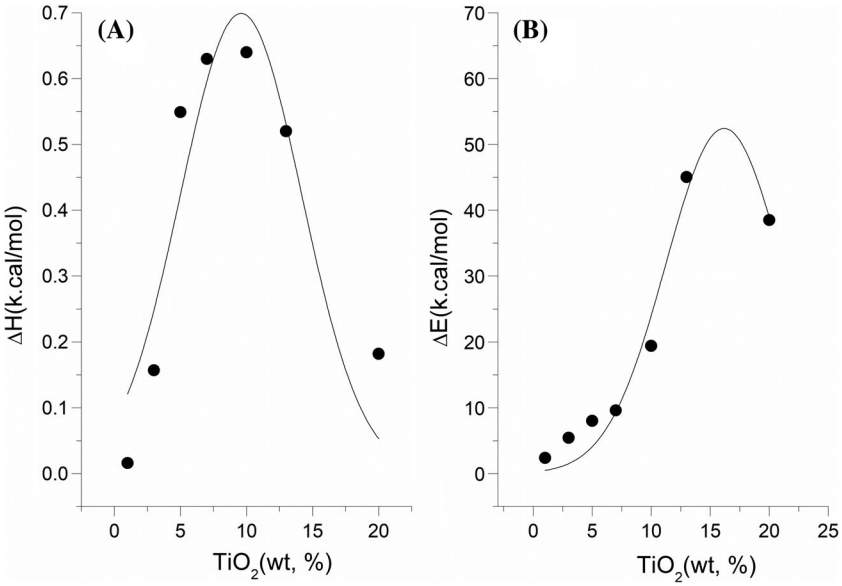


FIGURE 10 The variation of the void closure (A), and the interdiffusion (B) activation energies with respect to the TiO_2 content for the annealed composite films

explains the interdiffusion processes since having high T_g of TiO_2 is more effective for the determination of ΔE values. At first, low TiO_2 contributed particles moves easily since there is no obstacle for the movement and can come together for the interaction. With the addition of TiO_2 particles, the situation of the replacement of the particles is having difficulty since becoming clusters in the matrix. Polymer chains have more free volume and less interaction between chain segments in high TiO_2 causing to higher conformational energy and less interaction of segments. The film is covered by TiO_2 particles after certain TiO_2 content and chain transfer is getting easier causes less energy to be completed of the interdiffusion processes.

The averaged ΔH and ΔE values were found to be as a maxima, 0.65 and 65 kcal/mol for the composite films, respectively. The activation energy of viscous flow, that is, the dependence of viscosity on temperature is determined by the structure of polymer chain. In other words, the type of branches and the presence of polar groups in the chain determine the kinetic flexibility of polymer. For carbon chain polymers, ΔH is found to be 5 to 7 kcal/mol (polyethylene). ΔH reaches to the value of 15 kcal/mol for PIB. For polystyrene whose side groups are phenyl rings, ΔH rises to 28 kcal/mol. For the long chain of polyvinylacetate, ΔE is 35 kcal/mol. Here, the obtained ΔH values are much smaller than that of examples. It is also seen that ΔE values are much higher than ΔH. It is quite reasonable that a single chain needs more energy to diffuse across the polymer-polymer interface than bulk polymer needs.

Healing, T_h, temperatures are plotted vs TiO_2 content in Figure 11, where T_h values increase above 3 wt% TiO_2 content. This behavior of T_h clearly indicates that the existence of TiO_2 delays the film formation process for the high amount of TiO_2.

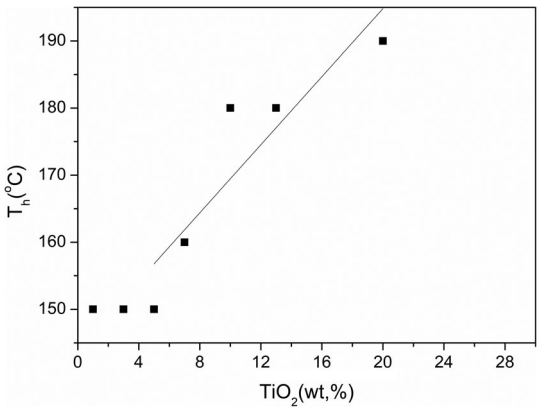


FIGURE 11 The variation of healing, T_h, temperatures with respect to the TiO_2 content for the composite films

Figure 12 shows the maxima of I_{tr} points during the annealing processes for different TiO_2 content films annealed at 150°C where I_{tr} values are decreasing for all films as can be seen in Figure 8. It is clearly seen that I_{tr} is decreasing with the addition of TiO_2 acting as scattering centers in the film. The composite film scatters high number of photons due to increase in the heterogeneity level of the film. Thus, the optical level becomes quite low due to obstruction of penetrating photons into the composite film.

4 | CONCLUSIONS

The effect of an opaque material TiO_2 which are especially used in the catalysts applications on a transparent

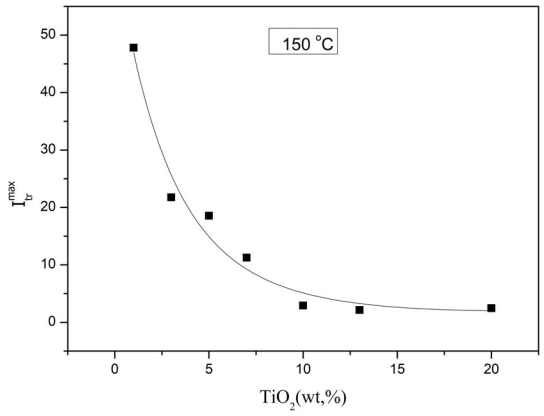


FIGURE 12 The variation of the maximum transmitted light intensity at 800 nm with respect to the TiO_2 content for the composite films

material PVA was investigated by photon transmission technique. The results showed the addition of the low content of TiO_2 delays the film formation process and requires more energy to be completed of void closure process. However, above the addition of 10 wt% TiO_2, the film formation is completed much easier and needs less energy for both the void closure and the interdiffusion process. In the mechanical measurements, the thermal stability effect was investigated in terms of the glass transition (T_g) affect by high-T_g of TiO_2 on the low-T_g of PVA. Annealing the composite films is considerably improved the mechanical stability of the composite films that the Young's modulus of 5 wt% TiO_2 has increased around 40 times at 150°C compared with that of unheated sample. This temperature value was also consistent with the optical measurements that above this temperature, the transmitted light intensity started to decrease for all composites which is the beginning of the interdiffusion process. From the results of the mechanical measurements, the tensile strength and the Young's modulus increased remarkably for the heating temperature increased up to 150°C for the lower content of TiO_2 such as 5 wt% whereas the strain at break values decreased significantly. However, with the increase of TiO_2 content up to 50 wt%, the heating temperature for which the mechanical strength and modulus increased shifted to 180°C. This is because the properties of thermal and mechanical stability of TiO_2 are much higher than those of PVA.

ACKNOWLEDGMENT

The authors acknowledge the financial support of Scientific Research Projects Coordinatorship in Yıldız Technical University in İstanbul, Turkey, through the Grant of the Project with the number of 2016-01-01-GEP02.

ORCID

Altan Bozdoğan https://orcid.org/0000-0002-6493-0210
Baki Aksakal https://orcid.org/0000-0003-1255-541X
Onder Yargi https://orcid.org/0000-0001-6343-0057

REFERENCES

[1] O. Yargi, A. Gelir, B. Sarli, U. Sahinturk, B. Aksakal, C. Denktas, *Prog. Org. Coat.* **2018**, *117*, 146.
[2] A. Gelir, O. Yargi, B. Sarli, U. Sahinturk, B. Aksakal, *Polym. Eng. Sci.* **2018**, *58*(3), 353.
[3] O. Yargi, A. Gelir, U. Sahinturk, T. Ozer, M. Caliskan, B. Aksakal, *Polym. Compos.* **2018**, *40*, E1441.
[4] O. Yargi, A. Gelir, M. Ozdogan, C. Nuhoglu, A. Elaissari, *J. Appl. Polym. Sci.* **2016**, *133*, 43289.
[5] D. Distler, G. Kanig, *Colloid Polym. Sci.* **1978**, *256*, 1052.
[6] Y. Wang, A. Kats, D. Juhue, M. A. Winnik, R. R. Shivers, C. J. Dinsdale, *Langmuir* **1992**, *8*, 25.
[7] B. J. Roulstone, M. C. Wilkinson, J. Hearn, A. J. Wilson, *Polym. Int.* **1991**, *24*(2), 87.
[8] K. D. Kim, L. H. Sperling, A. Klein, G. D. Wignall, *Macromolecules* **1993**, *26*, 4624.
[9] O. Pekcan, M. A. Winnik, M. D. Croucher, *Macromolecules* **1990**, *23*, 2673.
[10] Y. Wang, C. Zhao, M. A. Winnik, *J. Chem. Phys.* **1991**, *95*, 2143.
[11] Y. Wang, M. A. Winnik, *Macromolecules* **1993**, *26*, 3147.
[12] Ö. Pekcan, M. Canpolat, *J. Appl. Polym. Sci.* **1996**, *59*(2), 277.
[13] Ö. Pekcan, M. Canpolat, A. Göçmen, *Polymer (Guildf.)* **1993**, *34*, 3319.
[14] M. Canpolat, Ö. Pekcan, *J. Polym. Sci., Part B: Polym. Phys.* **1996**, *34*(4), 691.
[15] E. Arda, V. Bulmuş, E. Pişkin, Ö. Pekcan, *J. Colloid Interface Sci.* **1999**, *213*(1), 160.
[16] Ö. Pekcan, E. Arda, *Colloids Surf., A* **1999**, *153*(1–3), 537.
[17] A. M. Shehap, K. A. Elsayed, D. S. Akil, *Phys. E (Amsterdam, Neth.)* **2017**, *86*, 1.
[18] X. Liu, Q. Chen, L. Lv, X. Feng, X. Meng, *Catal. Commun.* **2015**, *58*, 30.
[19] S. Sugumaran, C. S. Bellan, *Optik (Munich, Ger.)* **2014**, *125*, 5128.
[20] V. Kaler, U. Pandel, R. K. Duchaniya, *Development of TiO_2/PVA Nanocomposites for Application in Solar Cells*, Vol. 5, Elsevier, Hyderabad, **2018**.
[21] U. Siemann, *Scattering Methods and the Properties of Polymer Materials*, Springer Berlin Heidelberg, Berlin, Heidelberg **2005**, p. 1.
[22] D. C. L. Vasconcelos, V. C. Costa, E. H. M. Nunes, A. C. S. Sabioni, M. Gasparon, W. L. Vasconcelos, *Mater. Sci. Appl.* **2011**, *2*, 1375.
[23] A. M. Shehap, D. S. Akil, *Int. J. Nanoelectron. Mater.* **2016**, *9*, 17.
[24] M. Sivabalan, V. Gayathri, C. Kiruthika, B. Madhan, *Int. J. Pharm. Technol.* **2012**, *4*, 4493.
[25] R. Singh, S. G. Kulkarni, S. S. Channe, *Polym. Bull.* **2013**, *70*, 1251.
[26] A. M. Shehap, *Egypt. J. Solids* **2008**, *31*(1), 75.
[27] J. Ahmad, K. Deshmukh, M. B. Hägg, *Int. J. Polym. Anal. Charact.* **2013**, *18*(4), 287.

[28] S. M. Pawde, K. Deshmukh, S. Parab, *J. Appl. Polym. Sci.* **2008**, *109*, 1328.
[29] S. M. Pawde, K. Deshmukh, *J. Appl. Polym. Sci.* **2008**, *109*, 3431.
[30] C. Linga Raju, J. Rao, B. Reddy, K. Veera Brahmam, *Bull. Mater. Sci.* **2007**, *30*(3), 215.
[31] B. Aksakal, Ö. Yargı, U. Şahinturk, *J. Appl. Polym. Sci.* **2017**, *134*, 44915.
[32] O. N. Tretinnikov, S. A. Zagorskaya, *J. Appl. Spectrosc.* **2012**, *79*, 521.
[33] M. Tsukada, G. Freddi, J. S. Crighton, *J. Polym. Sci., Part B: Polym. Phys.* **1994**, *32*(2), 243.
[34] E. A. El-Hefian, M. M. Nasef, A. H. Yahaya, *E-J. Chem.* **2011**, *8* (1), 91.
[35] W. A. Jabbar, N. F. Habubi, S. S. Chiad, *J. Arkansas Acad. Sci.* **2010**, *64*, 101.
[36] S. Mallakpour, N. Jarang, *J. Plast. Film Sheeting* **2016**, *32* (3), 293.
[37] S. Mallakpour, V. Behranvand, *Colloid Polym. Sci.* **2014**, *292*, 2857.
[38] N. B. Rithin Kumar, V. Crasta, R. F. Bhajantri, B. M. Praveen, *J. Polym.* **2014**, *2014*, 1.
[39] J. F. Kenney, G. W. Willcockson, *J. Polym. Sci., Part A-1: Polym. Chem.* **1966**, *4*(3), 679.
[40] S. Mahendia, K. G. Heena, U. P. Deshpande, S. Kumar, *J. Mol. Struct.* **2016**, *1111*, 46.
[41] G. Attia, M. F. H. Abd El-Kader, *Int. J. Electrochem. Sci.* **2013**, *8*, 5672.
[42] X. Chen, *J. Mater. Sci. Lett.* **2002**, *21*, 1637.
[43] E. J. Shin, Y. H. Lee, S. C. Choi, *J. Appl. Polym. Sci* **2004**, *91*, 2407.
[44] L. Dai, J. Li, E. Yamada, *J. Appl. Polym. Sci.* **2002**, *86*, 2342.
[45] A. Danno, *J. Phys. Soc. Jpn.* **1958**, *13*(6), 609.
[46] S. Krimm, C. Y. Liang, G. B. B. M. Sutherland, *J. Polym. Sci.* **1956**, *22*(101), 227.
[47] I. Korbag, S. Mohamed Saleh, *Int. J. Environ. Stud.* **2016**, *73* (2), 226.
[48] K. S. Chan, H. B. Senin, I. Naimah, M. Rusop, T. Soga, *AIP Conference Proceedings*, Vol. 1136, AIP, Selangor, **2009**, p. 366.
[49] P. Sakellariou, A. Hassan, R. C. Rowe, *Colloid Polym. Sci.* **1993**, *271*, 1083.
[50] E. F. dos Reis, F. S. Campos, A. P. Lage, R. C. Leite, L. G. Heneine, W. L. Vasconcelos, Z. I. P. Lobato, H. S. Mansur, *Mater. Res.* **2006**, *9*(2), 185.
[51] N. Chen, J. Zhang, *Chin. J. Polym. Sci.* **2010**, *28*(6), 903.
[52] Y. Lou, M. Liu, X. Miao, L. Zhang, X. Wang, *Polym. Compos.* **2009**, *31*, 1184.
[53] E. Džunuzović, K. Jeremić, J. M. Nedeljković, *Eur. Polym. J.* **2007**, *43*, 3719.
[54] D. Jiang, Y. Xu, B. Hou, D. Wu, Y. Sun, *J. Solid State Chem.* **2007**, *180*, 1787.
[55] C. F. Cheng, H. H. Cheng, P. W. Cheng, Y. J. Lee, *Macromolecules* **2006**, *39*, 7583.

How to cite this article: Bozdoğan A, Aksakal B, Yargi O. Film formation and mechanical properties of an opaque titanium dioxide and transparent polyvinyl alcohol composite films. *Polymer Composites*. 2019;1–12. https://doi.org/10.1002/pc.25425